

AD-A111 340

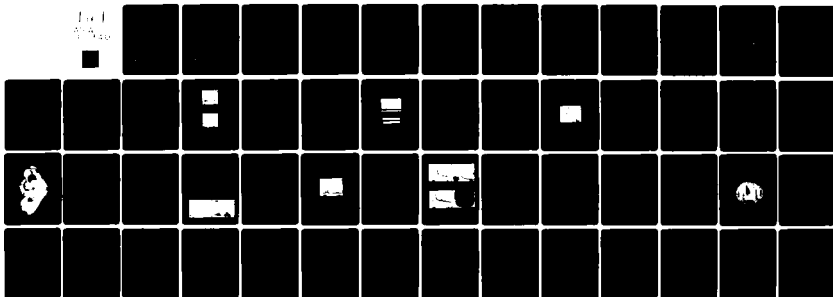
SANDERS ASSOCIATES INC NASHUA NH DEFENSIVE SYSTEMS DIV  
EYESAFE LASER TRANSCIEVER.(U)  
NOV 81 M G KNIGHTS

F/6 20/5

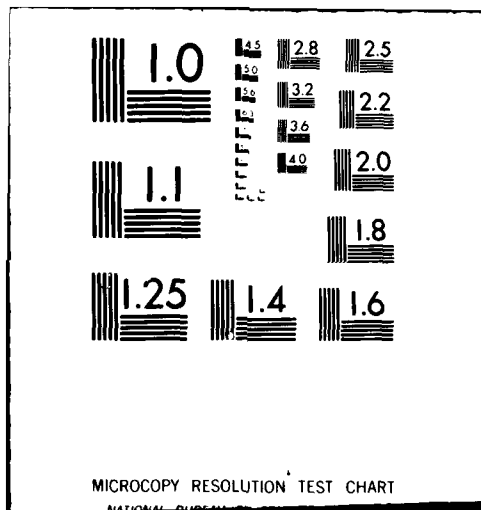
UNCLASSIFIED

DAAK20-79-C-0034  
NL

1 of 1  
10/1/82



END  
DATE  
FILMED  
3-82  
DTIC



MICROCOPY RESOLUTION TEST CHART  
NATIONAL BUREAU OF STANDARDS-1963-A

AD A111340

**EYESAFE  
LASER  
TRANSCEIVER**

Final Report For:  
September 1979 - July 1981  
CONTRACT DAAK20-79-C-0034

Prepared For:  
**U.S. Army Electronics Research and  
Development Command  
Fort Belvoir, VA 22060**

DTIC  
ELECTE  
FEB 26 1982  
S A D

Prepared by:  
Defensive Systems Division  
Federal Systems Group  
 **SANDERS**  
95 CANAL STREET - NASHUA, NEW HAMPSHIRE 03061

This document has been approved  
for public release and sale; its  
distribution is unlimited.

DTIC FILE COPY

82 02 25 057

---

# **EYESAFE LASER TRANSCEIVER**

**Final Report For:  
September 1979 - July 1981  
CONTRACT DAAK20-79-C-0034**

**Prepared For:  
U.S. Army Electronics Research and  
Development Command  
Fort Belvoir, VA 22060**

**Prepared by:**  
Defensive Systems Division  
Federal Systems Group  
 **SANDERS**  
95 CANAL STREET · NASHUA, NEW HAMPSHIRE 03061

---

UNCLASSIFIED

SECURITY CLASSIFICATION OF THIS PAGE (When Data Entered)

REPORT DOCUMENTATION PAGE		READ INSTRUCTIONS BEFORE COMPLETING FORM
1. REPORT NUMBER <b>AD-A111 340</b>	2. GOVT ACCESSION NO.	3. RECIPIENT'S CATALOG NUMBER
4. TITLE (and Subtitle) <b>EYESAFE LASER TRANSCEIVER</b>		5. TYPE OF REPORT & PERIOD COVERED <b>FINAL Sept 1979 - July 1981</b>
7. AUTHOR(s) <b>M. G. Knights</b>		6. PERFORMING ORG. REPORT NUMBER
8. PERFORMING ORGANIZATION NAME AND ADDRESS <b>Sanders Associates, Inc. Defensive Systems Division 95 Canal St., Nashua, NH 03061</b>		9. CONTRACT OR GRANT NUMBER(s) <b>DAAK20-79-C-0034</b>
11. CONTROLLING OFFICE NAME AND ADDRESS <b>US Army Night Vision &amp; Electro-optics Laboratory ATTN: DELNY-L (Bulova)  Ft. Belvoir, VA 22060</b>		10. PROGRAM ELEMENT, PROJECT, TASK AREA & WORK UNIT NUMBERS
14. MONITORING AGENCY NAME & ADDRESS (if different from Controlling Office)		12. REPORT DATE <b>November 1981</b>
		13. NUMBER OF PAGES
		15. SECURITY CLASS. (of this report) <b>Unclassified</b>
		16a. DECLASSIFICATION/DOWNGRADING SCHEDULE
16. DISTRIBUTION STATEMENT (of this Report)		
<div style="border: 1px solid black; padding: 5px; width: fit-content; margin: auto;"> <p>This document has been approved for public release and sale; its distribution is unlimited.</p> </div>		
17. DISTRIBUTION STATEMENT (of the abstract entered in Block 20, if different from Report)		
18. SUPPLEMENTARY NOTES		
19. KEY WORDS (Continue on reverse side if necessary and identify by block number) <b>Rare Earth Lasers Er:YLF Eyesafe Lasers</b>		
20. ABSTRACT (Continue on reverse side if necessary and identify by block number) <b>This final report details the work carried out to design, fabricate and test a brassboard 1.73<math>\mu</math>m eyesafe transceiver. The objective of the program was to develop a compact, efficient 1.73<math>\mu</math>m Er:YLF laser and to couple the laser to a Germanium photodiode receiver.</b>		

*Caution*

~~SECURITY CLASSIFICATION OF THIS PAGE (When Data Entered)~~

On this program 10-30mJ of Q-switched 1.730 $\mu$ m laser output was obtained, for pump energies of 20-30 Joules, from a compact Er:YLF laser. Repetitively pulsed Q-switched laser operation was maintained for 10 seconds without significant loss of output. The laser was coupled to a germanium photodiode receiver and ranging was demonstrated, with high S/N to a variety of non-cooperative targets at ranges of 1-2Km; projected ranging capability is 4-5Km. The brassboard transceiver was delivered to the Night Vision Laboratory.



~~SECURITY CLASSIFICATION OF THIS PAGE (When Data Entered)~~

FOREWORD

This report was prepared by Sanders Associates, Inc., Nashua, New Hampshire under contract DAAK20-79-C-0034. The work was funded by ERADCOM and was administered under the direction of the Night Vision Laboratory, Fort Belvoir, VA. Mr. Richard Bulava was the project monitor.

This is the final technical report for contract DAAK20-70-C-0034. It covers the period from September 1979 to July 1981. The report was submitted in November 1981.

Section For	
CS&I	<input checked="" type="checkbox"/>
TIB	<input type="checkbox"/>
Advanced	<input type="checkbox"/>
Application	
<i>Item 50</i>	
<i>on file</i>	
Distribution/	
Availability Codes	
and/or	
Special	
<i>A</i>	

## TABLE OF CONTENTS

	<u>Page</u>
1.0 SUMMARY	1
1.1 Introduction	1
1.2 Background	1
1.3 Results	2
2.0 TECHNICAL DISCUSSION	3
2.1 General	3
2.2 Laser Transmitter	3
2.2.1 1.73 $\mu$ m Laser Transition	3
2.2.2 Laser Design	3
2.2.3 1.73 $\mu$ m Laser Performance	7
2.2.4 1.73 $\mu$ m Laser: Summary	10
2.3 Laser Drive Electronics	13
2.3.1 Pulse Forming Network (PFN)	13
2.3.2 Flashlamp Trigger Circuit	13
2.3.3 Q-switch Crowbar	16
2.3.4 Summary: Laser Firing Sequence	16
2.4 1.73 $\mu$ m Receiver/Optics	17
2.5 System Packaging	19
2.6 Summary	22
3.0 RANGE DATA	23
3.1 Hard Targets	23
3.2 Multiple Returns/Clutter	25
3.3 Summary	26
4.0 SUMMARY AND RECOMMENDATIONS	29
APPENDIX I EYE SAFETY CONSIDERATIONS	31
APPENDIX II EYESAFE LASER TRANSCIVER OPERATIONS AND ALIGNMENT	40

## TABLE OF FIGURES

<u>FIGURE #</u>	<u>TITLE</u>	<u>PAGE</u>
1	Er:YLF 1.73 $\mu$ m Laser Transition	4
2	Brewster Laser Schematic	5
3	Brewster Resonator Performance	8
4	1.73 $\mu$ m Q-switched Pulse	9
5	Repetitively Pulsed Performance	11
6	Q-switched Operation: Repetitively Pulsed	12
7	Flashlamp Pulse Forming Network	14
8	Flashlamp Light Output: Temporal Profile 20 $\mu$ s/Horizontal Division	15
9	Transceiver Optics	18
10	Eyesafe Transceiver System	20
11	Transceiver Layout	21
12	Return Pulses: Hard Targets	23
13	Return Pulses: Hard Targets	23
14	Light Baffle Placement	24
15	Return Pulse: Hard Target	25
16	Return Pulse: Vegetation	27
17	Multiple Returns: Vegetation	27
18	Multiple Returns: Building & Vegetation	27
19	Return Pulse: Clouds	27
20	Calculated Range Performance	28

## SECTION 1.0 SUMMARY

### 1.1 INTRODUCTION

The results of a program to design, fabricate and test a brassboard 1.73 $\mu$ m eyesafe laser transceiver are presented in this document. The objective of the program was to develop a relatively compact and efficient laser utilizing the 1.73 $\mu$ m transition in Erbium doped Lithium Yttrium Fluoride (Er<sup>3+</sup>:YLF), and to couple the laser to a Germanium photodiode receiver. This work was carried out under contract DAAK20-79-C-0034.

Specific program goals were as follows:

- i) Laser efficiency: 10mJ Q-switched output, at 1.73 $\mu$ m, for a laser size and pump energy commensurate with a compact device.
- ii) Laser output pulsewidth:  $\leq 150$ ns FWHM
- iii) Laser operation: 1Hz operation, uncooled, for a duty cycle to be determined.
- iv) Output beam divergence:  $< 2$ mR
- v) Fabrication and delivery of the transmit/receive components as a single brassboard assembly with optics aligned.

### 1.2 BACKGROUND

The development of eyesafe systems is dependent upon the selection of a laser which emits in the spectral region,  $\lambda > 1.4\mu$ m. In this region corneal absorption limits the power density at the

retina, where damage thresholds are lowest. Because of the large volume of absorbing material in the cornea, relatively high fluences may be accommodated before the onset of eye damage. Parameters relating to laser induced eye damage are discussed in detail in Appendix I.

Sanders' eyesafe laser technology is based on the crystalline solid laser material  $\text{Er}^{3+}:\text{YLF}$  (Erbium doped Lithium Yttrium Fluoride,  $\text{LiYF}_4$ ). The  $1.73\mu\text{m}$  laser transition in  $\text{Er}:\text{YLF}$  was first operated in 1972 at Sanders Associates. The laser exhibits the low threshold characteristic of four-level transitions, is easily Q-switched and is in band to low cost germanium photodiodes. Sanders specific approach on this program was to couple a 10mJ,  $1.73\mu\text{m}$  laser to a germanium photodiode receiver.

### 1.3 RESULTS

The following results were obtained on this program.

- 10-30mJ of Q-switched  $1.73\mu\text{m}$  laser output was obtained, for pump energies of 20-30 Joules, from a compact  $\text{Er}:\text{YLF}$  laser.
- Repetitively pulsed Q-switched operation at 1 Hz was maintained for 10 seconds without significant loss of output.
- With a 3" receiver aperture, ranging was demonstrated with high S/N to a variety of non-cooperative targets at ranges of 1-2Km; projected ranging capability is 4-5Km.
- A brassboard transceiver was designed, fabricated and delivered to the Night Vision Laboratory.

## 2.0 TECHNICAL DISCUSSION

### 2.1 GENERAL

The eyesafe laser transceiver consists of a 1.73 $\mu$ m Q-switched laser, Germanium photodiode receiver and associated electronics. With the exception of charging supply and control circuitry all components are contained within the main transceiver housing. The transceiver requires a 24/15 volt power supply and logic-level trigger pulse; output consists of analog  $t_0$  and target return pulses. This section details the design and construction of each of the above subsystems - laser, receiver, electronics - as well as the packaging of the integrated transceiver assembly. Transceiver alignment and operation are detailed in Appendix II.

### 2.2 LASER TRANSMITTER

#### 2.2.1 1.73 $\mu$ m Laser Transition

The 1.73 $\mu$ m laser utilizes the  $^4S_{3/2} \rightarrow ^4I_{9/2}$  transition of trivalent erbium in lithium yttrium fluoride ( $Er^{3+}$ :YLF). The relevant energy levels are shown in Figure 1. This transition is four-level, the lower laser level being located some 12,000 $cm^{-1}$  above the ground state. The upper laser level is fed rapidly via multiphonon relaxation from the pump bands, which extend from the green region of the visible spectrum into the near-ultraviolet. Due to rapid population of the upper laser level the transition is readily Q-switched, and multiple pulsing in the Q-switched mode is non-existent with careful laser design.

#### 2.2.2 Laser Design

The layout of the 1.73 $\mu$ m laser head is illustrated in Figure 2. The laser utilizes a 5 x 60mm Brewster angle  $Er$ :YLF rod, Lithium Niobate Q-switch and dielectric mirrors coated for 100% and 90%.

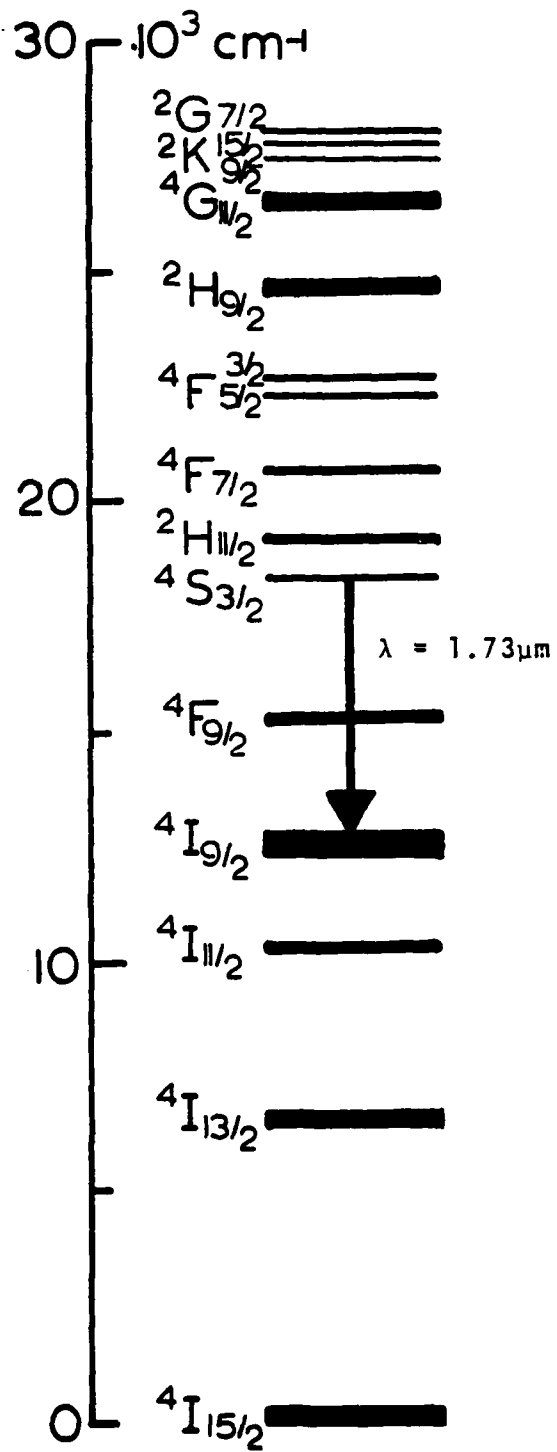


Figure 1  
Er:YLF 1.73 $\mu\text{m}$  Laser Transition

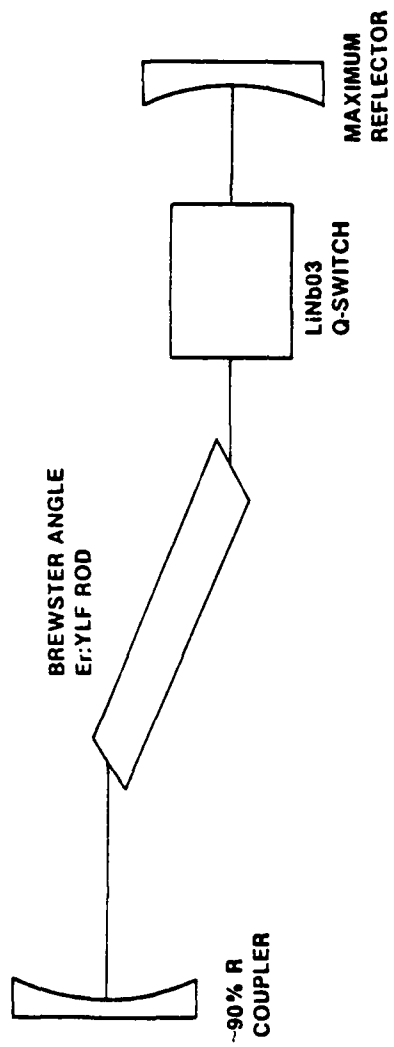


Figure 2  
Brewster Laser Schematic

reflectivity at  $1.73\mu\text{m}$ . The mirror separation is approximately 30cm and, with 30cm mirror radii, a stable confocal resonator is formed which is relatively alignment-insensitive.

The Brewster angle laser rod ends are oriented with respect to the rod c-axis such that:

i)  $1.73\mu\text{m}$  fluorescence and laser emission (which are plane polarized parallel to the c-axis) "see" Brewster's angle at the rod faces and thus reflection losses vanish. Antireflection coatings are therefore unnecessary.

ii) Circulating radiation whose polarization vector has been rotated  $90^\circ$  from the c-axis plane (during the pumping interval, with Q-switch electrified) is effectively ejected from the resonator by the Brewster faces, as the reflection loss for this polarization is nearly 20% per face. The Brewster ends therefore eliminate the need for an intracavity polarizer for Q-switched operation.

The  $\text{Er}^{3+}$ :YLF rod is pumped by a Xenon flashlamp in a close-coupled polished aluminum cavity. The  $100\mu\text{s}$  flashlamp pulse is initiated by series injection triggering; optimal Q-switch crowbar timing was experimentally determined to be  $95\mu\text{s}$  after initiation of the lamp pulse.

The  $9 \times 9 \times 25\text{mm}$  Lithium Niobate pockels cell requires a potential difference of 3750 volts for  $1/4$  wave rotation at  $1.73\mu\text{m}$ . The low gain nature of the laser, however, eases the Q-switch electrical requirements, in that full  $1/4$  wave retardation is not required of the switch to hold off the laser gain during pumping. A 1.9KV potential difference across the crystal was determined to be adequate to hold off lasing. In addition to the holdoff voltage, a d.c. bias of approximately 25% of the Q-switch voltage is employed

to counter the piezoelectric "ringing" effects inherent in Lithium Niobate Q-switches. The resultant voltage levels needed are thus a 2.5KV switching voltage and 0.6KV bias voltage. No multiple-pulsing or post lasing was observed using this Q-switching arrangement.

### 2.2.3 1.73 $\mu$ m Laser Performance

Slope efficiency data for the 1.73 $\mu$ m laser described above are illustrated in Figure 3. Included are data for long pulse operation (laser rod and mirrors only), long pulse operation with inactive Lithium Niobate inserted, and Q-switched operation. From the data it is apparent that two losses are involved in Q-switching the Er:YLF laser. The first loss is an insertion loss encountered upon placing the Q-switch crystal, inactive, into the laser resonator. With 90% coupling reflectivity the reduction in laser output varies from 30% - 50% upon insertion of the switch, and appears to be dependent on both crystal face AR coatings and upon bulk crystal quality (principally birefringence inhomogeneities in the material). The second loss appears in actually switching the laser and is due to the finite lifetime (and thus energy storage capability) of the laser material. In spite of these losses, however, Q-switched outputs of 10-15mJ are readily obtainable at flashlamp inputs of ~25 Joules. A typical Q-switched pulse is illustrated in Figure 4; Q-switch opening (as indicated by the electrical noise on the oscilloscope trace) is followed in approximately 300ns by the onset of the laser pulse. The risetime of the pulse, 10% - 90%, is 100ns and the pulsewidth is approximately 150ns FWHM. These pulse shapes were recorded using a high speed pyroelectric probe and storage oscilloscope.

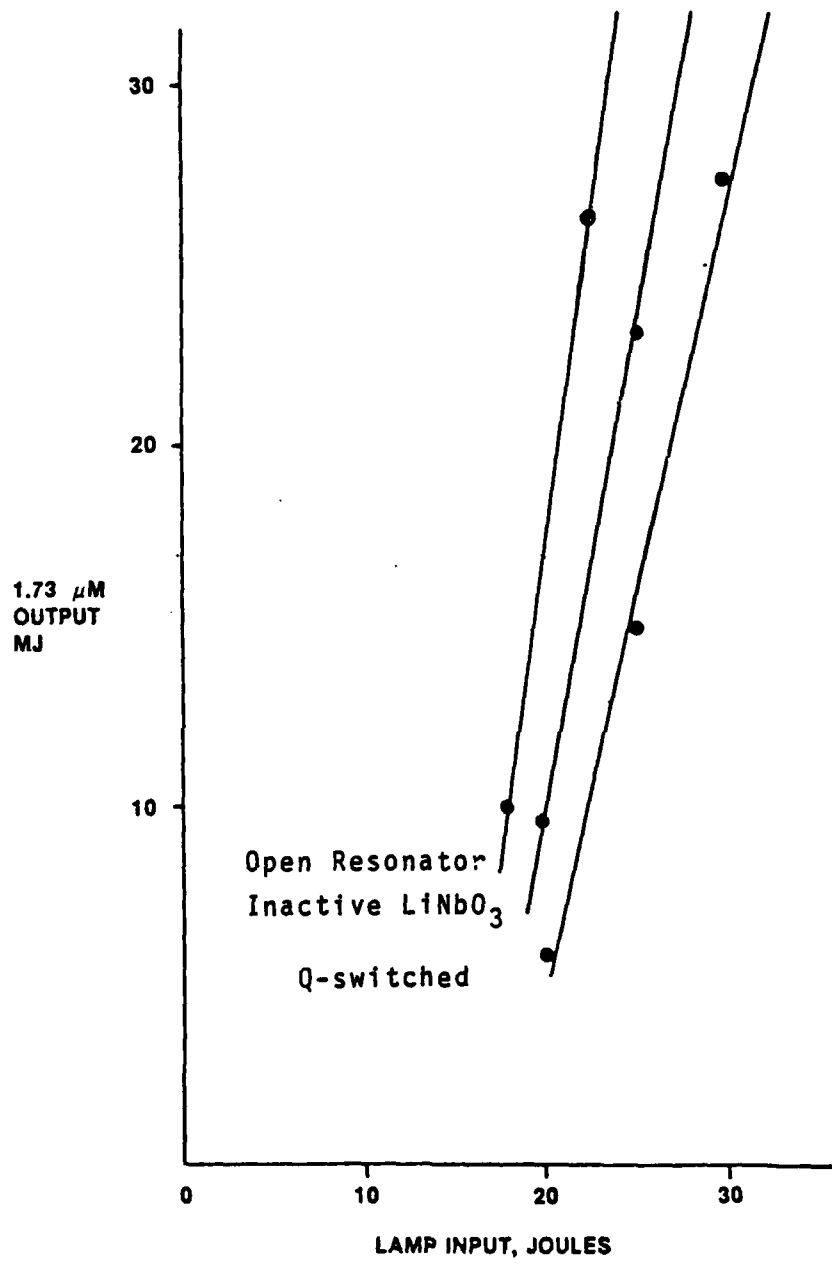


Figure 3  
Brewster Resonator Performance

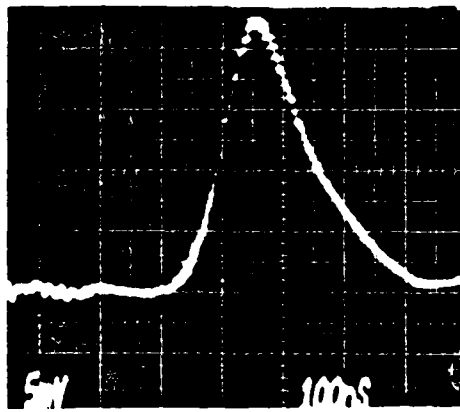
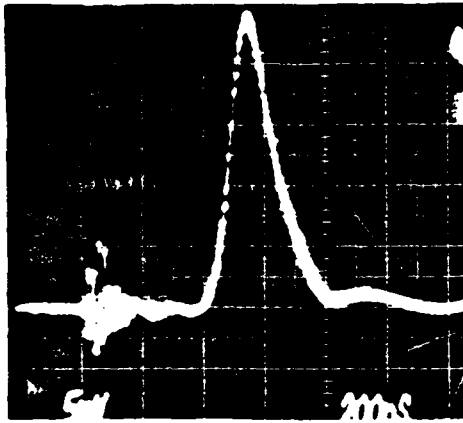


Figure 4  
1.73 $\mu$ m Q-switched Pulse

Repetitively pulsed (unswitched) laser performance at 1Hz is illustrated in Figure 5. Flashlamp input was adjusted to yield a laser output of ~15mJ; a pulse generator was then used to trigger the lamp at one-second intervals. The laser output was measured with a Scientech power/energy meter coupled to an x-y plotter. Plotter output depicts the laser energy versus the number of shots taken: the initial rise is principally due to the response time of the power meter/plotter; output of the laser remains approximately constant at 15mJ for 20 pulses, before beginning a slow timewise decline. No form of cooling was employed during this test.

A series of ten Q-switched laser pulses taken at 1Hz is shown in Figure 6. In this case the laser output was monitored with a germanium photodiode and storage oscilloscope. A slow timewise degradation again appears in the data; the effect, however, is slight: after 10 pulses the output energy is still at ~85% of its initial value. Also shown in Figure 6 are polaroid burn patterns obtained from 10 consecutive Q-switched shots at 1Hz. These were taken approximately 1 inch in front of the laser output mirror, and appear quite uniform throughout the series of shots, reflecting only the slow decline of output energy with time.

#### 2.2.4 1.73 $\mu$ m Laser: Summary

A 1.73 $\mu$ m laser was designed and fabricated for use in the brassboard transceiver. The laser employs a 5 x 60mm Brewster-angle laser rod and 30cm confocal resonator. Q-switching is accomplished via a Lithium Niobate pockels cell, and 150ns FWHM pulses of 10-15mJ are readily obtained for lamp inputs of 20-25 Joules. The device may be operated in a repetitively pulsed uncooled mode, and 1Hz operation for 10 seconds was demonstrated without appreciable degradation of laser output energy or beam quality.

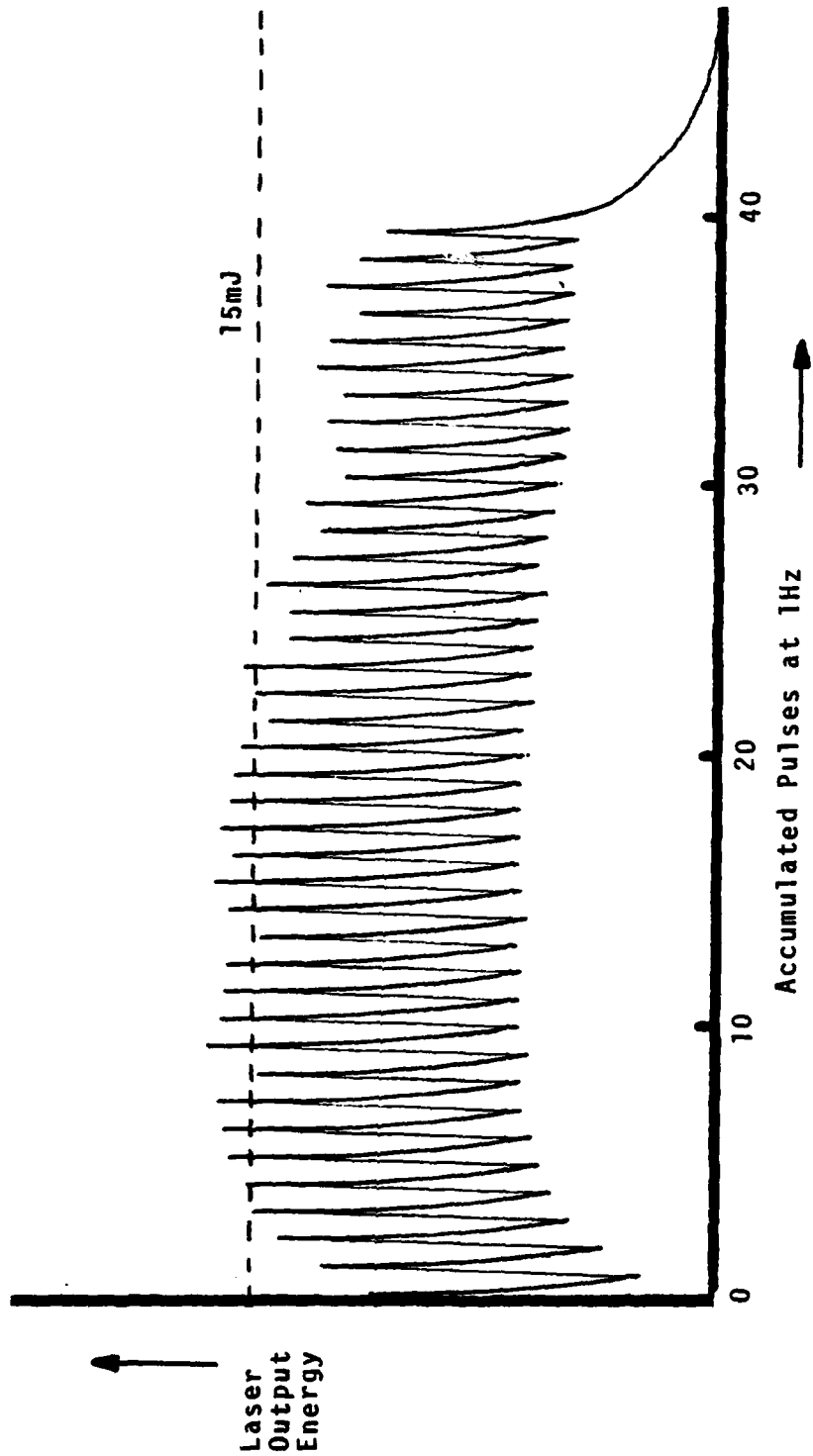


Figure 5  
Repetitively Pulsed Performance

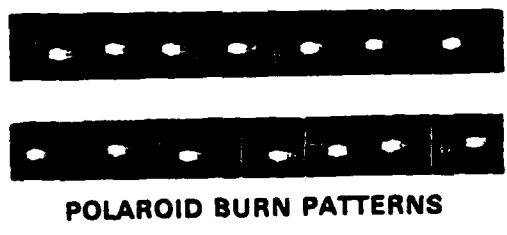
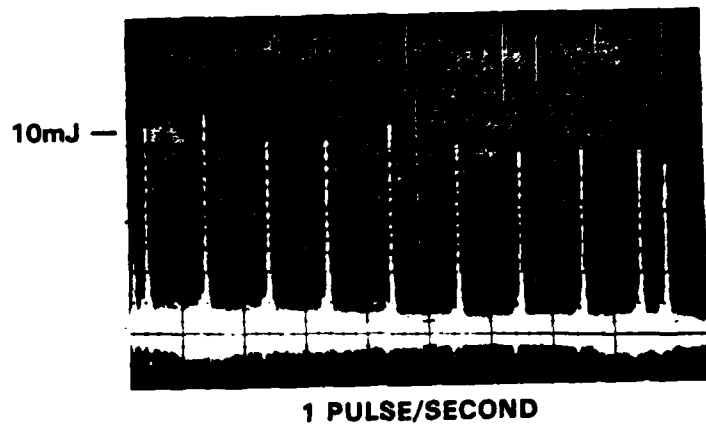


Figure 6  
Q-Switched Operation: Repetitively Pulsed

## 2.3 LASER DRIVE ELECTRONICS

The laser drive electronics are comprised of the flashlamp pulse forming network, flashlamp trigger circuit, Q-switch crowbar circuit, and high voltage power supply for the capacitor bank and pockels cell.

The high voltage power supply was purchased for this application as a self contained unit. The high voltage power supply package requires a 24VDC input and logic level control voltages, and provides the pockels cell high voltage and bias (variable to 4200 and 1000 volts, respectively) as well as the capacitor charging voltage (variable to 1500 volts, at a 30 watt charging rate).

The pulse forming network, flashlamp trigger circuit and Q-switch crowbar circuit were fabricated at Sanders Associates. Each is described below.

### 2.3.1 Pulse Forming Network (PFN)

The flashlamp PFN employs a single mesh LCR circuit, as shown in Figure 7. The inductance is provided by the secondary winding of the series injection trigger transformer. At a 25 Joule input the PFN delivers a current pulse to the lamp of  $\sim 100\mu\text{s}$  duration (10% points); the resultant flashlamp light output is illustrated in Figure 8. The flashlamp output with respect to time was obtained from a silicon photodiode and storage oscilloscope.

### 2.3.2 Flashlamp Trigger Circuit

The flashlamp is series triggered by the large potential difference which appears across the secondary winding of the trigger transformer, when a low voltage pulse is applied to the primary. This pulse is obtained by switching a charged capacitor across the

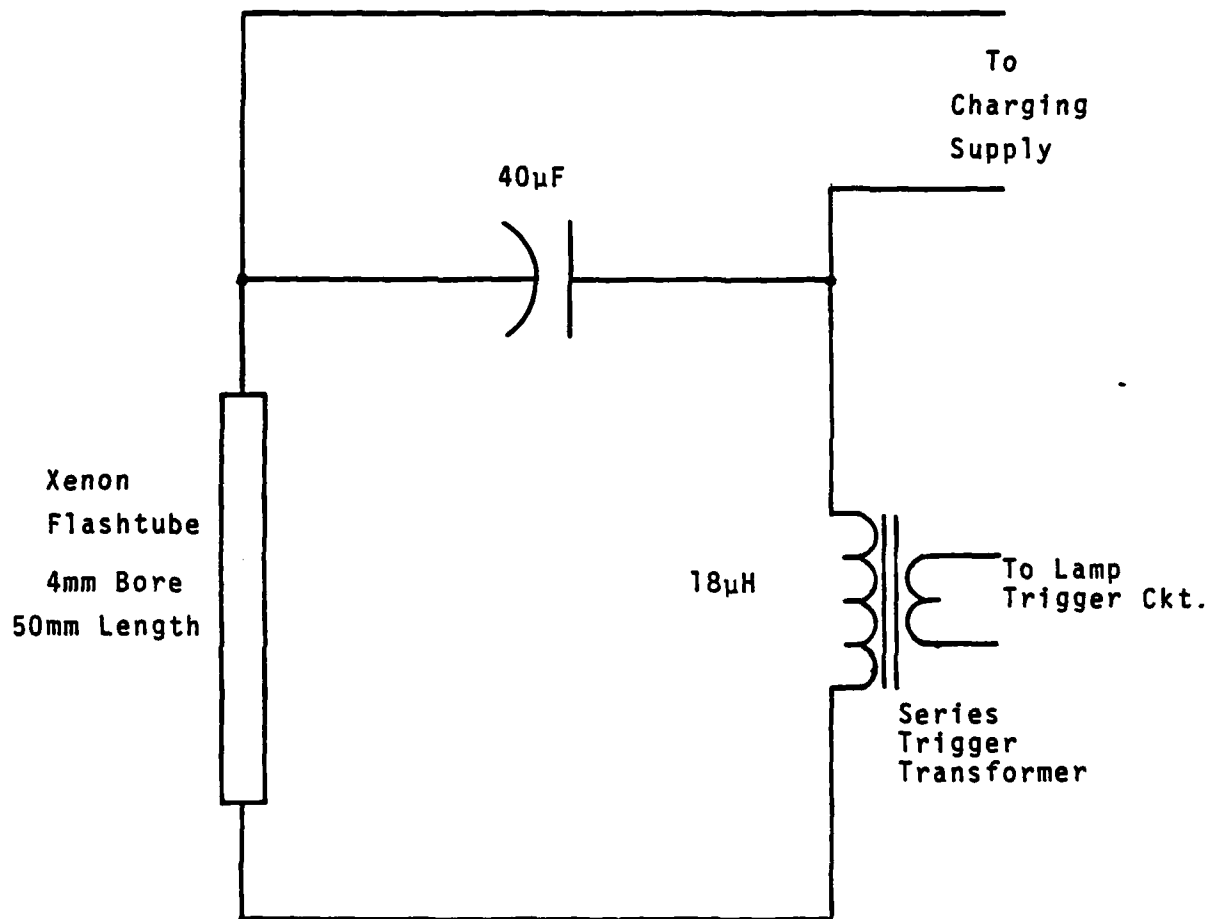


Figure 7  
Flashlamp Pulse Forming Network

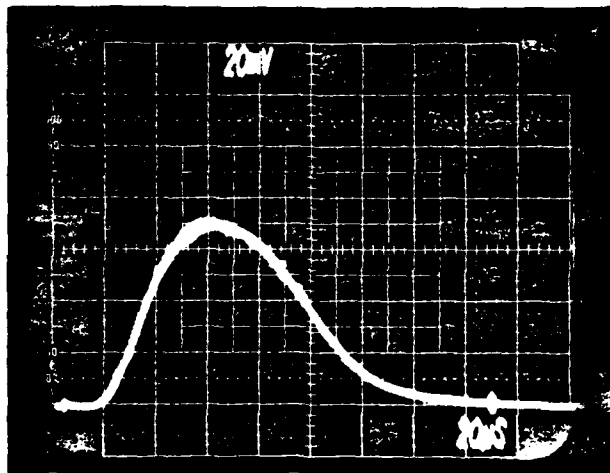


Figure 8  
Flashlamp Light Output: Temporal Profile  
20μs/Horizontal Division

primary winding with a Krytron cold-cathode switching tube. The primary (low voltage) pulse is typically 1250 volts; with a 10:1 turns ratio, a potential difference of 12.5KV appears across the secondary winding of the transformer. This has proven to be ample for reliably triggering the flashtube.

### 2.3.3 Q-switch Crowbar

The Q-switch crowbar circuit utilizes a counter, which is adjusted to provide the required delay time from the onset of the flashlamp pulse, and a Krytron switch to short the high voltage side of the pockels cell to ground and "open" the switch.

The switching delay counter is adjustable from 0-290 $\mu$ s, and consists of a digital register which "counts" to 256 ( $2^8$ ) at the rate of one count per 1.14 $\mu$ s, driven by an external clock. Counting begins at the onset of the lamp firing and ends when the register is full; at this time the Krytron switch is triggered to open the Q-switch. Adjustments in delay time are effected by "preloading" the register; the greater the number stored, the fewer clock cycles are required to fill the register, resulting in a shortened delay time.

### 2.3.4 Summary: Laser Firing Sequence

To fire the laser, the drive electronics described above are operated in the following sequence: the capacitor bank charge and Q-switch voltages are applied by furnishing "enable" logic - level voltages to the power supply. These charge and Q-switch enables are switched on manually by the operator; as long as the power supply is enabled, the capacitor bank and Q-switch voltages recharge immediately after each firing.

When the capacitor bank and Q-switch voltages are at operating levels the laser is fired by application of a 5-volt pulse to the trigger input connection. This pulse fires the lamp trigger Krytron and, as previously described, causes a 12.5KV potential to appear across the trigger transformer secondary winding (and the flashlamp). The lamp then triggers and the capacitor delivers its stored energy to the resulting arc.

The 5-volt initial trigger pulse is delivered simultaneously to the lamp trigger and Q-switch counter. Thus, when the lamp triggers, the register begins counting from its preset level; when the register "full" condition is reached the Q-switch crowbar is triggered, the pockels cell "opens" and the Q-switched laser pulse is emitted.

#### 2.4 1.73 $\mu$ m RECEIVER/OPTICS

The brassboard transceiver employs a receiver optical train which is coaxial to the transmitter beam forming optics. A schematic drawing of the optics is shown in Figure 9. The glass objective is 90mm in diameter, with a 200mm focal length. The central 34mm diameter of this lens acts as the final element in the transmitter beam forming optical train. The remainder of the lens is employed as the receiver objective; the receiver aperture area (54.4cm<sup>2</sup>) is thus roughly equal to that of an 85mm diameter collector. The transmitter and receiver optical paths are separated by a perforated, gold-coated flat mirror.

The transmitter beam forming optics serve two functions:

- i) Expansion of the output beam to reduce exit fluence to  $E_{\text{exit}} < 10\text{mJ/cm}^2$ . (ANSI Maximum Permissible Exposure).

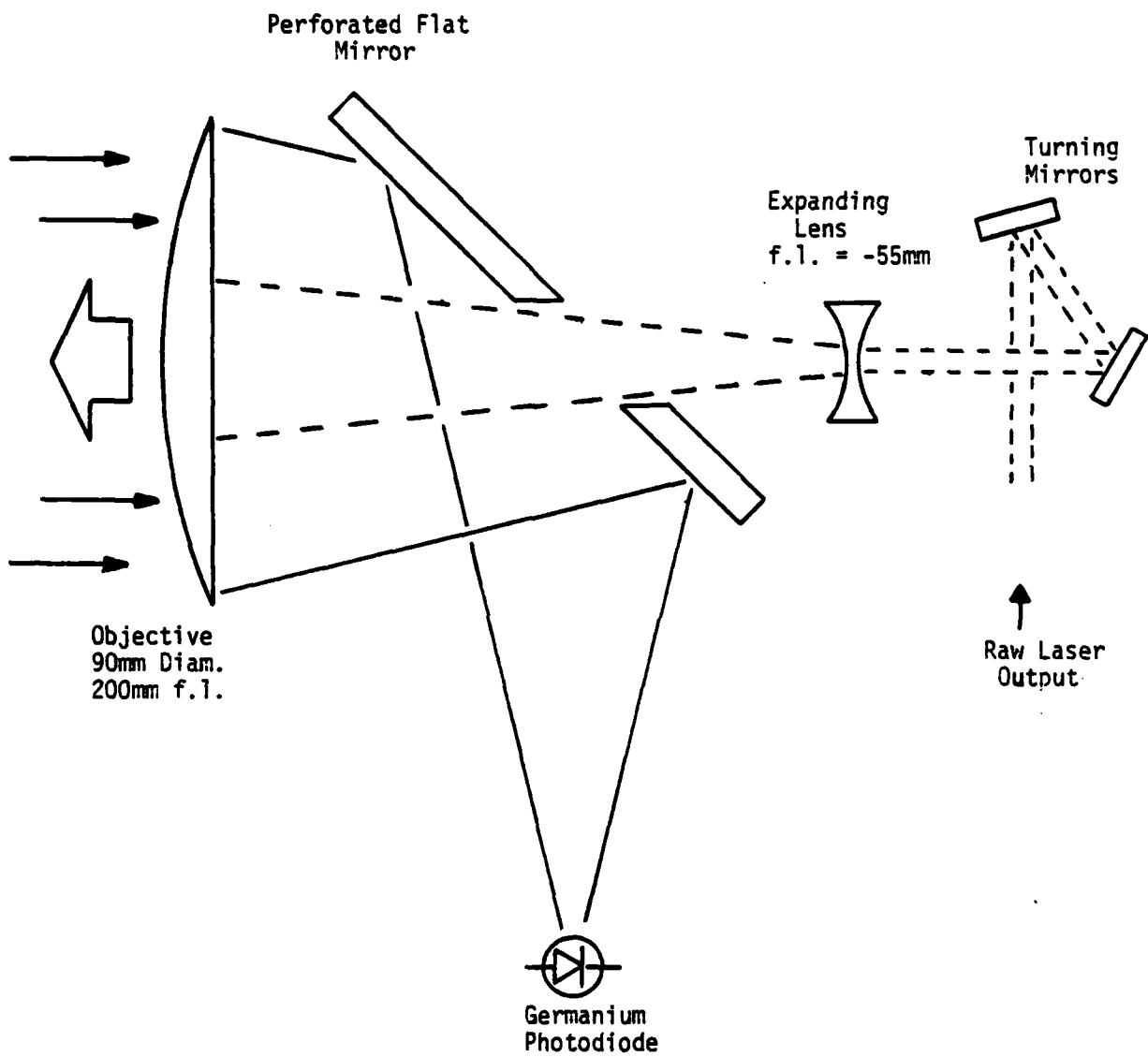


FIGURE 9  
TRANSCEIVER OPTICS

ii) Collimation of the expanded beam at reduced divergence.

The beam expander is a simple two-element telescope, with a negative lens located approximately 150mm in front of the laser coupling mirror, and positive recollimating element (the central portion of the receiver objective) equidistant and affixed to the transceiver front plate. The calculated beam divergence of the laser/beam expander combination is 2 milliradians (99% energy points). This divergence was verified in the field by scanning the 1.73 $\mu$ m beam at a distance of 2.5km. Measured beam diameter at this range was 4m, indicating a divergence of 1.6mR.

The plano-convex receiver objective focuses returned radiation onto a 1mm diameter germanium photodiode, via the perforated gold turning mirror (Figure 9). The receiver objective focuses 100% of the radiation into a diameter equivalent to the detector diameter, with 90% of the radiation in a 0.75mm diameter.

The germanium photodiode utilized in the receiver exhibits a typical pulsed responsivity of 0.15 A/W at 1.73 $\mu$ m. The diode is coupled to a 3 stage transistor preamplifier with an effective transimpedance of 12K $\Omega$ . The diode/preamplifier noise, at the output, is approximately 50 $\mu$ V; the minimum detectable incident power is thus about 25nW.

## 2.5 SYSTEM PACKAGING

Packaging of the 1.73 $\mu$ m transceiver system is shown pictorially in Figure 10 and schematically in Figure 11. The 1.73 $\mu$ m laser output beam is turned 90<sup>0</sup> via the gimballed gold turning mirrors and routed through the negative beam expanding lens, perforated flat mirror



FIGURE 10

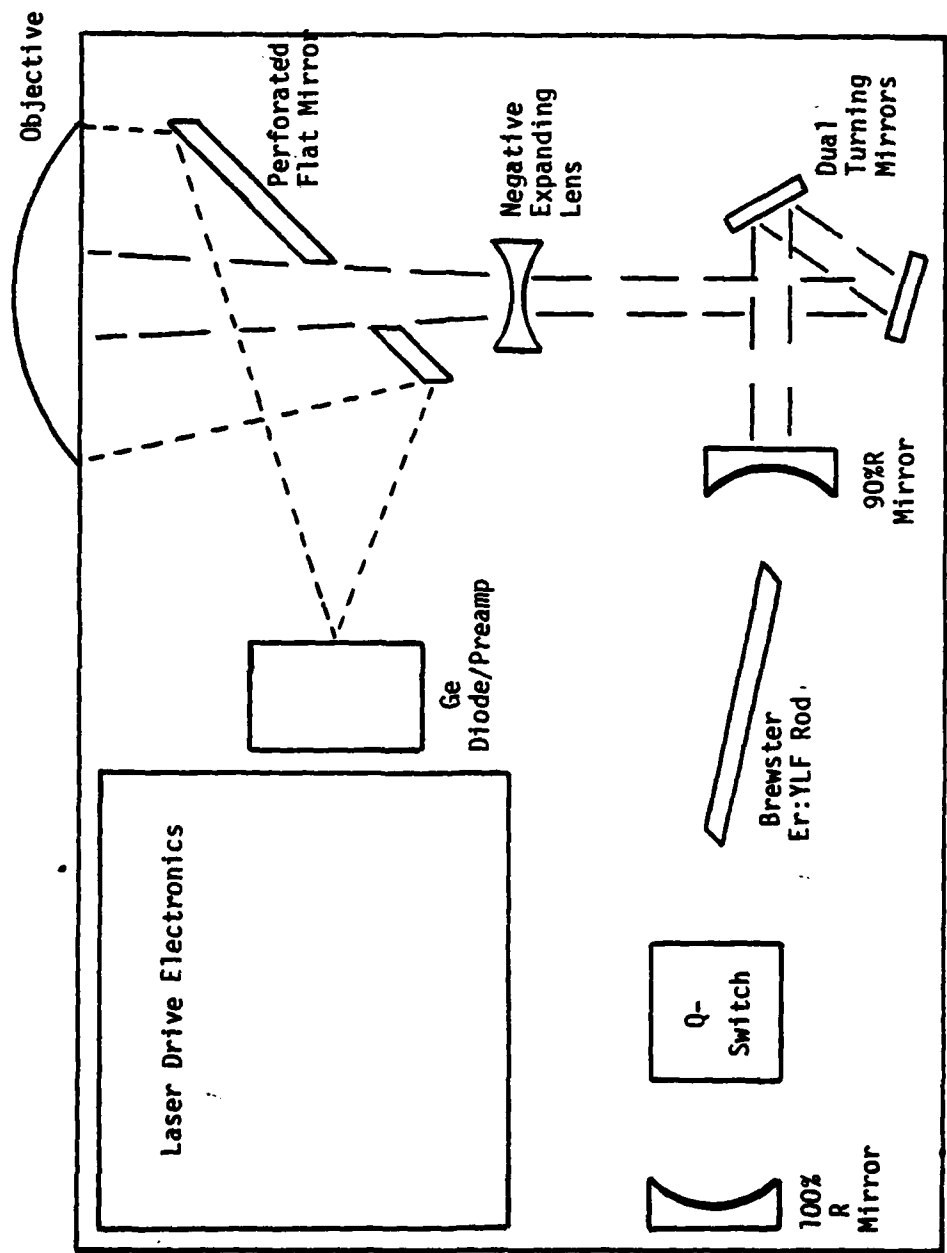


FIGURE 11  
TRANSCIEVER LAYOUT

and objective lens. The dual turning mirrors provide sufficient freedom to boresight the output beam to the receiver axis and sighting telescope. Both the receiver diode package and sighting telescope have adjustments as well, for fine tuning of the boresight alignment.

The laser drive electronics are housed within the aluminum enclosure adjacent to the laser head. This housing isolates these electronic assemblies from the laser head and eases possible RFI problems. The flashlamp trigger circuit, lamp PFN, Q-switch crowbar circuit and Q-switch timing card are located within this enclosure; the PFN charging power supply and controls are external and connected via cable.

Overall transceiver assembly dimensions are 10.40 x 16.50 x 5.875 inches, yielding a volume of approximately 0.6ft<sup>3</sup>.

## 2.6 SUMMARY

A transceiver has been constructed utilizing a 1.73 $\mu$ m Er<sup>3+</sup>:YLF laser and germanium photodiode receiver. The laser, receiver, coaxial optics, and laser drive electronics are packaged as a single assembly of approximately 0.6 ft<sup>3</sup> volume. A separate enclosure contains the power supply and control circuitry. The transceiver emits 10mJ at 1.73 $\mu$ m in a 150ns FWHM pulse, with a transmit beam diameter/divergence of 34mm/1.6mR. The receiver employs 54cm<sup>2</sup> of collecting aperture, and utilizes a biased germanium photodiode coupled to a high gain, low noise preamplifier.

The system requires power inputs and a logic level "fire" pulse. The output consists of analog  $t_0$  and target return pulses and is suitable for inspection using a high speed oscilloscope.

Range data acquired in transceiver testing is presented in the following section.

### 3.0 RANGE DATA

A limited amount of range data was collected to ensure that the transceiver was properly aligned and to check the operation of the various subassemblies. In all cases the transmitter output was in the 6-10mJ range, depending upon the laser duty cycle used in obtaining the data.

Representative range data is presented below, in the form of oscilloscope traces containing the  $t_0$  (outgoing) pulse and target returns. A high speed oscilloscope with storage capability was used to record the signals. Pertinent conditions are listed with the signal traces.

#### 3.1 HARD TARGETS

Initially, several non-cooperative hard targets were ranged. At this time, the magnitude of the  $t_0$  signal ( $\sim 2.5V$ ) indicated a need for internal baffling to more effectively isolate the outgoing signal from the receiver optics. Figures 12 and 13 illustrate the  $t_0$  and return pulses, for a range building and construction trailer located at approximately 840 and 500 meters, respectively.

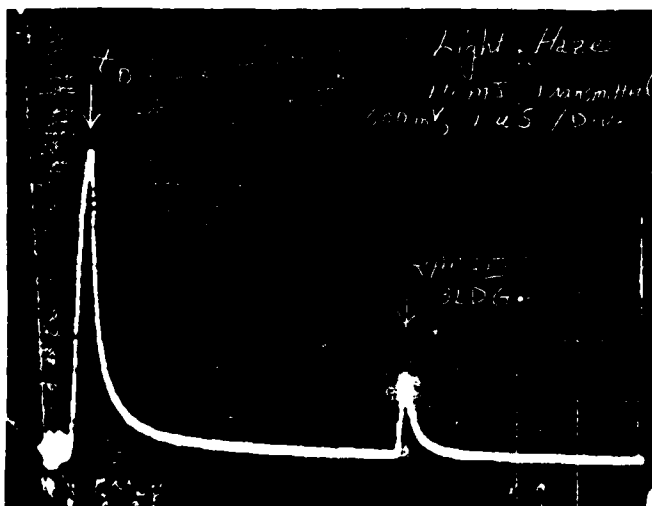


Figure 12

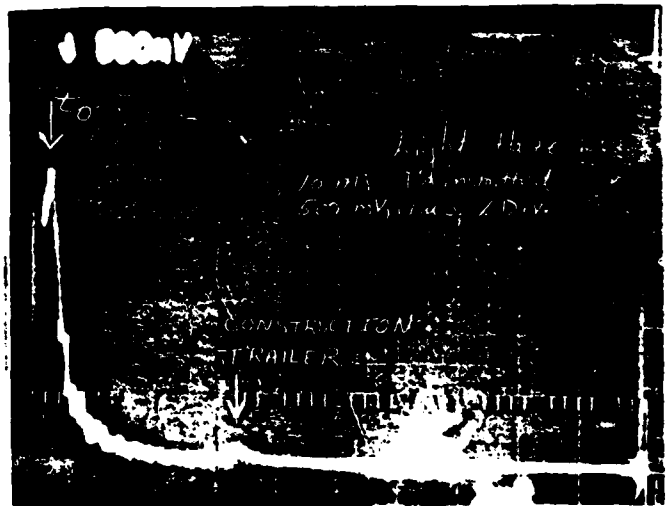


Figure 13

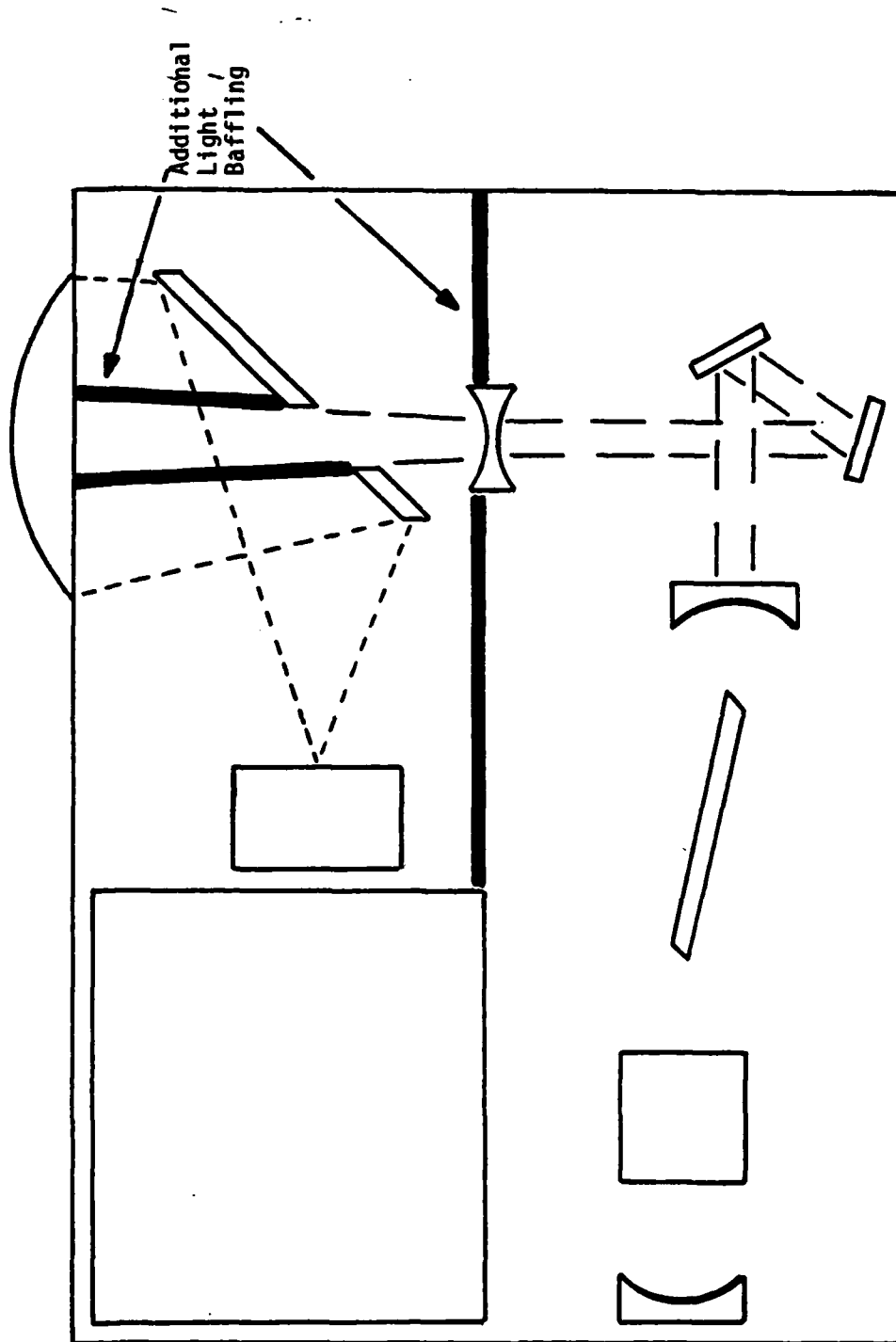


FIGURE 14  
LIGHT BAFFLE PLACEMENT

Baffling was installed to isolate the laser head from the receiver optics and to isolate the transmit beam from the coaxial return path within the transceiver. Figure 14 illustrates the placement of the baffles. Installation of the light baffles reduced the magnitude of the  $t_0$  pulse to approximately 300mV. Figure 15 shows a range shot obtained from a radome at 300 meters; the marked reduction in  $t_0$  pulse magnitude is apparent.

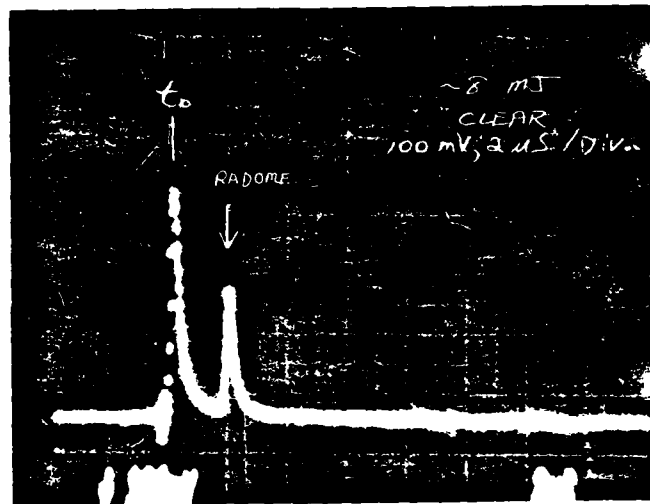


Figure 15

### 3.2 MULTIPLE RETURNS/CLUTTER

The reduction in  $t_0$  pulse amplitude enabled ranging to more distant/less reflective objects, in that oscilloscope input saturation (on the  $t_0$  pulse) was no longer problematic. Several range shots were made to vegetation at various distances; these are illustrated in Figures 16-18. Figure 16 depicts the  $t_0$  and return pulses from vegetation at 1.6Km. Figure 17 illustrates multiple returns from vegetation at 0.5 and 1.8Km. Figure 18 contains a strong return from a range building at 840m, followed by a second return from vegetation approximately 550m beyond.

A final piece of range data was obtained by turning the transceiver skyward: Figure 19 shows a return from a cumulus cloud at 1.7Km. With a receiver rms noise level of approximately  $50\mu\text{V}$ , this trace indicates a signal to noise ratio of about 5:1 from this rather "soft" diffuse target.

### 3.3 SUMMARY

Both hard and soft non-cooperative targets have been ranged at distances of up to ~2Km, limited by the test range available. Receiver noise was minimal (~ $50\mu\text{V}$  typically) and in all cases was contained within the width of the oscilloscope trace. Figure 20 illustrates the calculated ranging capability of the transceiver under several conditions of atmospheric visibility. The range calculations indicate a projected range capability of 4-5Km in clear conditions.

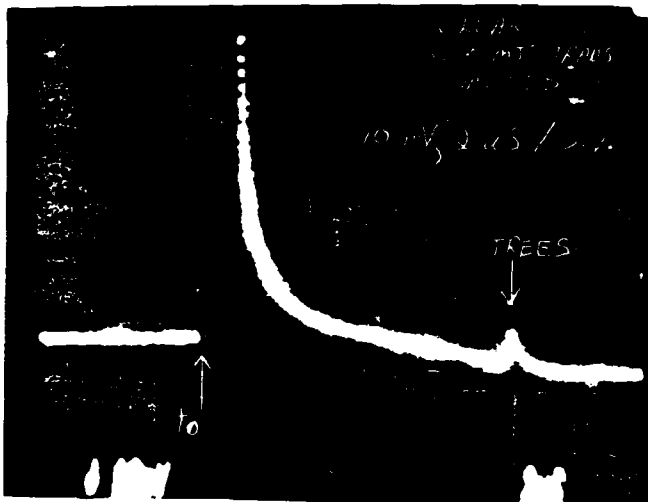


Figure 16

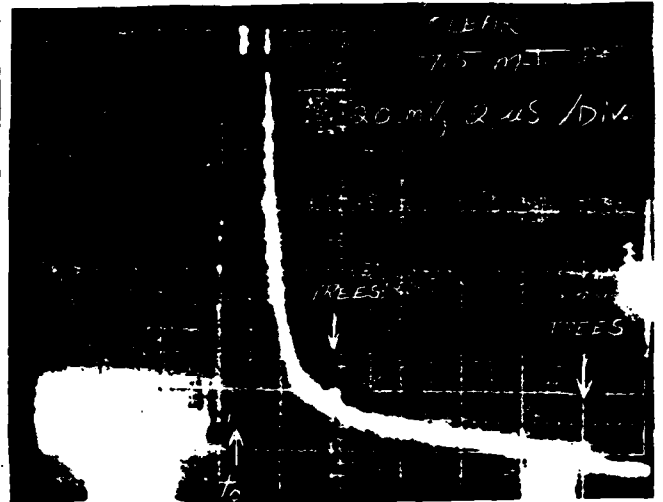


Figure 17

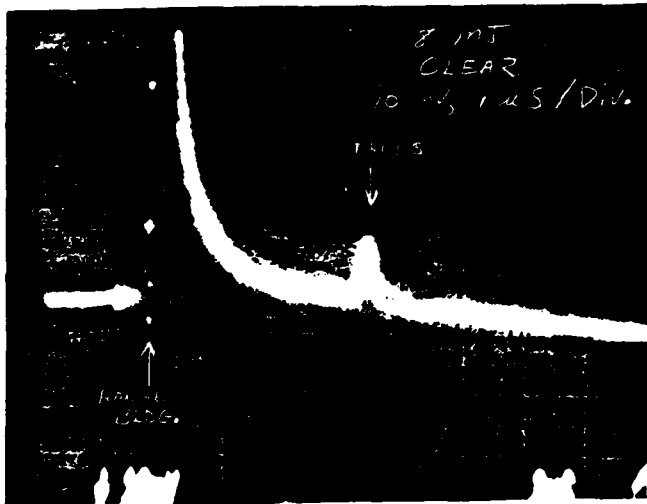


Figure 18



Figure 19

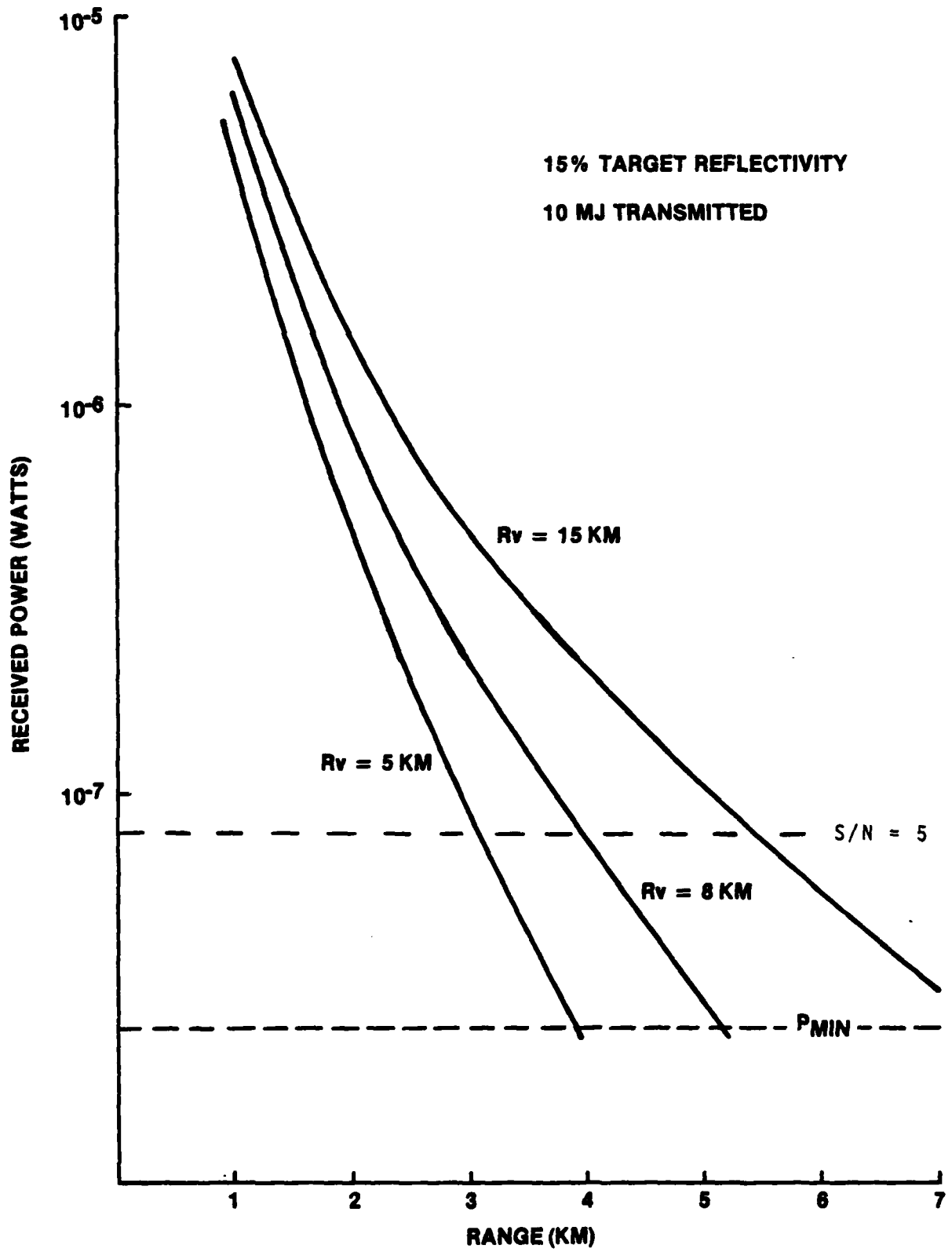


FIGURE 20  
CALCULATED RANGE PERFORMANCE

#### 4.0 SUMMARY AND RECOMMENDATIONS

The feasibility of a relatively compact brassboard eyesafe laser transceiver has been demonstrated on this program. Specific results obtained on the program were:

i) Design and fabrication of a compact 1.73 $\mu$ m laser capable of:

- 10mJ/pulse Q-switched output
- $\leq 150$ ns FWHM pulsewidth
- 1 Hz operation for 10 seconds without appreciable output degradation
- $< 2$ mR output beam divergence

ii) Fabrication of a germanium photodiode receiver and high gain transimpedance amplifier

iii) Packaging of the 1.73 $\mu$ m laser and receiver as a brassboard transceiver assembly

iv) Testing of the completed unit: ranging to non-cooperative targets at (test range limited) distances of 1-2 Km was demonstrated with high signal to noise ratio. The transceiver was subsequently delivered to the Night Vision Laboratory.

Future work in the eyesafe rangefinder area should be addressed to the following issues, grouped generally under laser and receiver:

LASER: Increased efficiency, primarily through improved Q-switching technology. The lithium niobate pockels cells used to switch the 1.73 $\mu$ m laser typically introduce a factor of 2 static loss in laser output. The loss is due to depolarization in the lithium niobate and to imperfect AR coatings on the crystal faces.

Solutions to this inefficiency include improved lithium niobate coatings, shorter crystals, and better quality crystals. A second laser Q-switching approach which must be explored is the use of acousto-optic switching devices; these are quartz, for which the coating technology is well advanced. With high damage resistance and low loss, a factor of two increase in laser efficiency may be attainable, provided an A-O switch yields sufficient loss to hold off lasing.

RECEIVER: Increased receiver responsivity directly affects ranging capability. Germanium photodiodes typically exhibit a NEP of  $\sim 10^{-11}$  W $\sqrt{\text{Hz}}$  in pulsed operation at 1.73 $\mu\text{m}$ . GaInAs photodiodes appear to offer a factor of 3-5 increase in responsivity; use of a GaInAs detector assembly should enable an immediate increase in receiver sensitivity.

Nearly another order of magnitude improvement in receiver sensitivity may be realized through development of microwave-biased germanium detector assemblies. Microwave biased detectors utilize a small microwave cavity containing a sample of photoconductive material such as germanium. Changes in sample conductivity (due to light absorption) vary the cavity Q, which is measurable to very high sensitivity. Microwave biased detectors were developed a decade ago, but have only recently become capable of compact packaging due to advances in microstrip cavities and RF oscillators. NEP's of  $\sim 2.5 \times 10^{-13}$  W $\sqrt{\text{Hz}}$  now appear practical from a device occupying a few cubic centimeters.

APPENDIX I  
EYE SAFETY CONSIDERATIONS

1.0 Introduction

The dangers of pulsed lasers to viewers of the laser beam are well known. There are several classes of ocular dangers from lasers of different wavelengths and powers, the most important of which, for minimizing risk, are those which occur at the lowest power levels. For the type of laser one anticipates for ranging applications (i.e. pulsed), the concerns are for (a) retinal burns and (b) damage to the cornea.

1.1 Retinal Damage

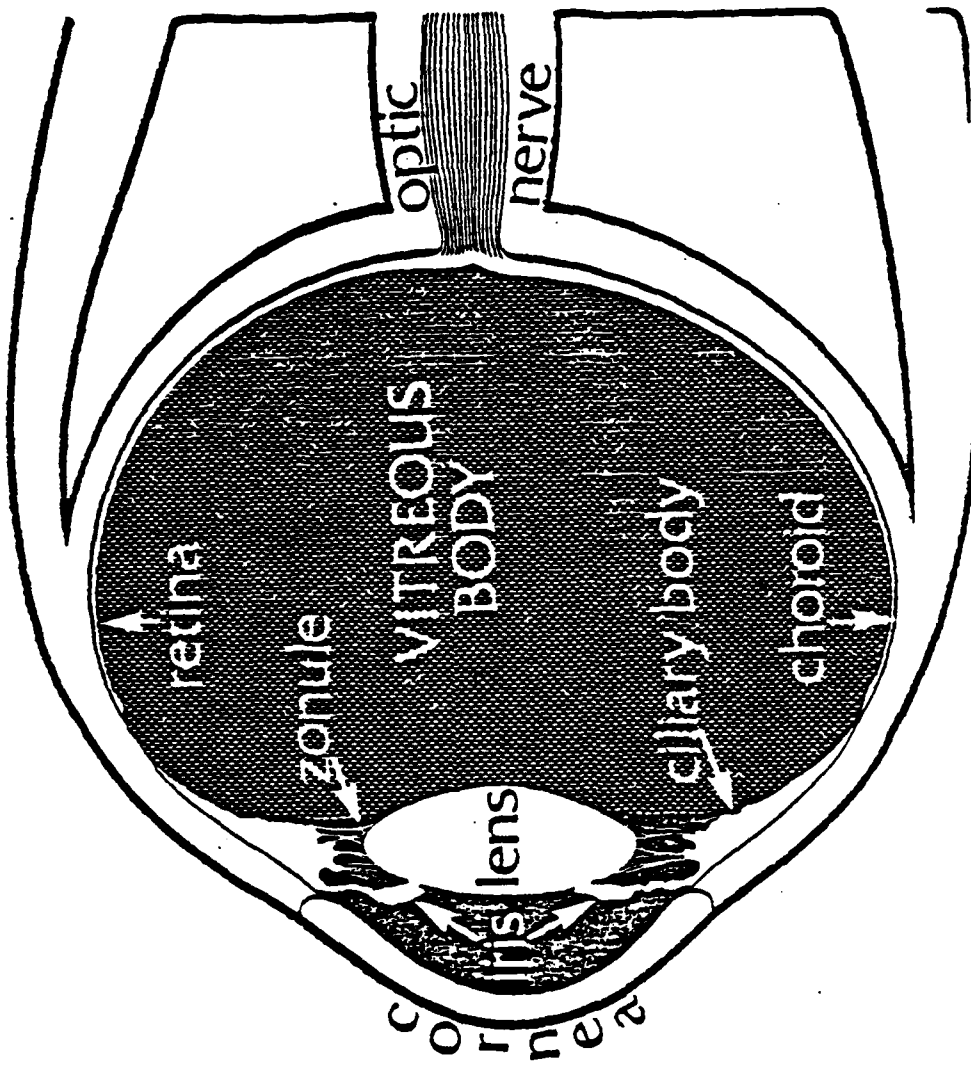
Figure 1 shows a diagram of the human eye. The cornea can be considered as a lens which focuses light from an object or source onto the retina, much in the way a camera lens images onto the film. Lasers are "dangerous" because they emit collimated light. This has two effects

- (a) the energy density at long ranges can be very high, and
- (b) the image size on the retina of a fully illuminated cornea can be very small

In addition to these properties, lasers can emit extremely high peak powers in short pulses which when focused onto the retina can generate retinal lesions. Two approaches have been recognized for assuring the retinal safety of lasers

- (a) operating at very low powers so that under "worst case" viewing conditions (optically aided observer at the exit aperture of the device), the total power at the retinal image is well below

# THE HUMAN EYE



the damage threshold, and

(b) preventing image formation at the retinal, by using a laser whose radiation is absorbed by the cornea (before it is focused to a higher power density).

The corneal fluid absorbs strongly beyond 1400nm and lasers for which  $\lambda > 1400\text{nm}$  are called "retinal safe".

## 1.2 Corneal Damage

Corneal damage can occur with "retinal safe" lasers, as the energy absorbed by the corneal fluid is converted into heat. Experiments have shown that when this fluid is heated to a temperature of about  $35^{\circ}\text{C}$  above ambient, irreversible biological damage occurs. The damage threshold then depends on the energy density at the cornea, and the absorption coefficient of the corneal fluid at the laser line.

It turns out that because of the concentration of the radiation, retinal damage always occurs at lower power levels when the laser wavelength is less than 1400nm. In the retinal safe region, corneal damage has been observed but at irradiance levels, orders of magnitude higher than retinal damage at  $\lambda < 1400\text{nm}$ . A detailed analysis with specific examples is presented below. This analysis was carried out by D.J. Lund of the Letterman Army Institute.

## 2 Calculated Damage Thresholds (D. J. Lund)

### 2.1 Model for Corneal Damage

From damage studies carried out with  $\text{CO}_2$  lasers ( $\lambda = 10.6\mu\text{m}$ ) it is known that when the corneal fluid is heated to about  $35^{\circ}\text{C}$  above

normal body temperature, irreversible damage occurs. Consider a slab of ocular fluid of area, A, and thickness dx. When this volume (A dx) is raised in temperature by a  $\Delta T = 35^{\circ}\text{C}$ , then damage will occur. The temperature rise (hence the risk) depends on wavelength since the absorption coefficient of the ocular fluid (water) is wavelength dependent.

Consider a plane wave  $I_0$  ( $\text{J}/\text{cm}^2$ ) incident as the disc characterized by an absorption coefficient  $\alpha$  ( $\text{cm}^{-1}$ ). In passing through this disc, the amount of energy deposited is given by

$$I_0 = 1 - e^{-\alpha dx}.$$

Since the specific heat of water is unity, we can write

$$A dx \Delta T = \frac{A}{4.186} [I_0 - I_0 e^{-\alpha dx}]$$

where 4.186 converts joules to calories, rearranging and expanding the exponential and neglecting higher powers of  $\alpha dx$  we have

$$A dx T \approx \frac{A I_0 dx}{4.186}$$

or

$$I_0 = \frac{4.186 \Delta T}{\alpha}$$

Figure B-2 shows the absorption coefficient for water. Sample calculations are summarized in Table 1, using  $\Delta T = 35^{\circ}\text{C}$  in the above expression.

FIGURE 2

J. A. CURCIO AND C. C. PETTY

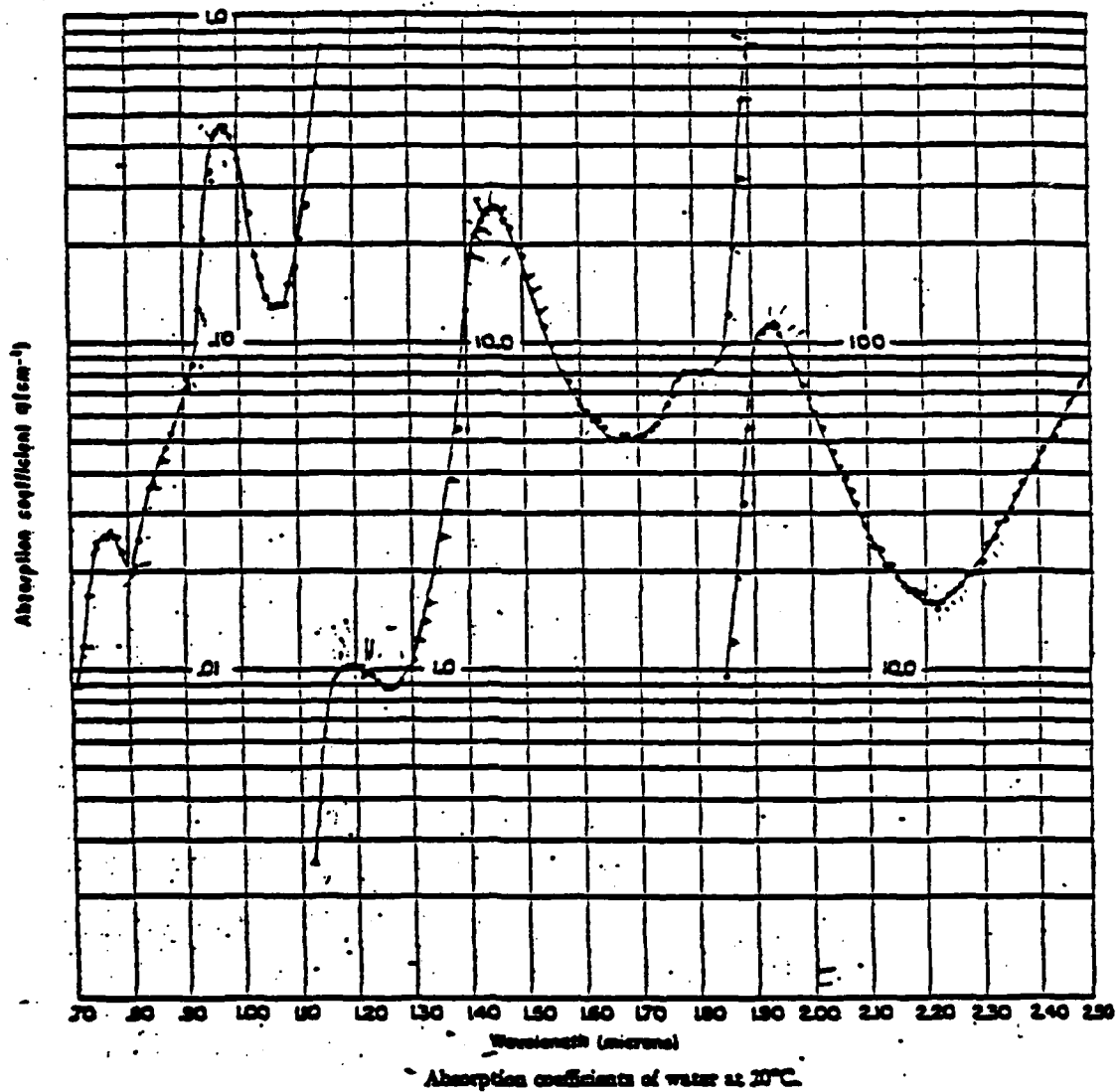


TABLE 1  
CORNEAL DAMAGE THRESHOLD

$\lambda$ (nm)	Ocular Absorption Coefficient $\text{cm}^{-1}$	Corneal Fluence for Corneal Damage (Joules/ $\text{cm}^2$ )
850	0.04	$3.7 \times 10^3$
904	0.07	$2.1 \times 10^3$
1064	0.15	$9.8 \times 10^2$
1330	1.5	100
1540	12	12
1730	6.5	22
2064	40	3.7

We see that the corneal damage threshold is immense even when the absorption coefficient is very high.

## 2.2 MODEL FOR RETINAL DAMAGE

In calculating the retinal damage threshold we assume the following:

Pupil diameter = 8 mm  
Retinal image diameter = 20 microns  
Intraocular path = 2.2cm.

The fluence at the retina is related to the incident fluence,  $I_0$ , by

$$I_{ret} = \frac{I_0 e^{-2.2\alpha} A_{pupil}}{A_{retina}}$$

where  $\alpha$  is the absorption coefficient and  $I_{ret}$  is the fluence at the retina.

$$I_{ret} = (1.6 \times 10^5) I_0 e^{-2.2\alpha}$$

Now for Q-switched ruby laser pulses retinal damage occurs at  $I_{ret} \approx 7 \times 10^{-2} \text{J/cm}^2$ . Assuming this is wavelength independent the prescription for retinal damage is then

$$I_0 = \frac{7 \times 10^{-2}}{1.6 \times 10^5} e^{2.2\alpha} = 4.4 \times 10^{-7} e^{2.2\alpha}$$

We see that once again the absorption coefficient of the ocular fluid is the determining factor. Using values of  $\alpha$  from Figure B-2 the corneal fluence for retinal damage is summarized below.

TABLE 2

## CORNEAL FLUENCE FOR RETINAL DAMAGE

Wavelength (nm)	Absorption Coefficient ( $\text{cm}^{-1}$ )	Corneal Fluence for Retinal <sub>2</sub> Damage $\text{J}/\text{cm}^2$
850	0.04	$5 \times 10^{-7}$
904	0.07	$5.1 \times 10^{-7}$
1064	0.15	$6 \times 10^{-7}$
1330	1.5	$1.2 \times 10^{-5}$
1540	12	$1.2 \times 10^5$
1730	6.5	0.7
2065	40	$7.2 \times 10^{31}$

We see that in the "eye safe" region ( $\lambda > 1400\text{nm}$ ) the calculated damage thresholds are immense. These estimates are in reasonable agreement with measurements carried out at the Letterman Army Institute.

At  $\lambda = 1540\text{nm}$  (Er:Glass) the measured threshold for corneal damage (Table 1) is  $20 \text{ J}/\text{cm}^2$  in good agreement with the calculated value of  $12 \text{ J}/\text{cm}^2$ . At 2064 (Ho: $\alpha$ BYLF) the measured damage threshold is  $2 \text{ J}/\text{cm}^2$  compared to the calculated value of 3.7.

### 3 ANSI AND BRH REGULATIONS

The American National Standards Institute (ANSI) and more recently the Bureau of Radiological Health (BRH) have issued regulations on lasers and laser products. The regulations are complicated and a complete discussion is beyond the scope of this discussion. We consider the case of a single Q-switched pulse of duration less than 100ns and compare the calculated damage thresholds with the "maximum

permissible exposure" of ANSI and the "accessible emission limit" of the BRH.

This comparison is shown in Table 3. The last column lists the margin provided by the BRH Class I regulations. It is the ratio of the calculated fluence at the cornea for corneal or retinal damage (whichever is smaller) to the exit fluence of a Class I laser. The exit fluence ( $\text{J}/\text{cm}^2$ ) is calculated by dividing the energy of a single pulse Q-switched laser by the area of an 80mm aperture.

We see from Table 3 that the safety margins in the eyesafe region are enormous. At 1730nm the ratio is  $4.4 \times 10^5$ !

TABLE 3  
EYE HAZARDS AND REGULATIONS<sup>1</sup>

Wavelength (nm)	Ocular Absorption Coefficient <sup>2</sup> (cm <sup>-1</sup> )	Calculated Corneal Fluence for Corneal Damage (J/cm <sup>2</sup> )	Calculated Corneal Fluence for Retinal Damage (J/cm <sup>2</sup> )	MPE <sup>3</sup> ANSI (J/cm <sup>2</sup> )	BRH <sup>4</sup> CLASS 1 FLUENCE 50.3 cm <sup>2</sup> Aperture (J/cm <sup>2</sup> )	MARGIN <sup>5</sup>
904	0.07	2.1 x 10 <sup>3</sup>	5.1 x 10 <sup>-7</sup>	1.3 x 10 <sup>-6</sup>	9.5 x 10 <sup>-9</sup>	54
1064	0.15	9.8 x 10 <sup>2</sup>	6 x 10 <sup>-7</sup>	5 x 10 <sup>-6</sup>	2 x 10 <sup>-8</sup>	30
1540	12	12 <sup>†</sup>	1.2 x 10 <sup>5</sup>	1*	1.57 x 10 <sup>-4*</sup>	7.6 x 10 <sup>4</sup>
1730	6.5	22	0.7	10 <sup>-2</sup>	1.57 x 10 <sup>-6</sup>	4.4 x 10 <sup>5</sup>
2065	40	3.7 <sup>††</sup>	7.2 x 10 <sup>31</sup>	10 <sup>-2</sup>	1.57 x 10 <sup>-6</sup>	2.3 x 10 <sup>6</sup>

<sup>1</sup> Single pulse laser, 1<100 ns

<sup>2</sup> Absorption coefficient of water at 20C (Curcio & Petty)

<sup>3</sup> Maximum Permissible Exposure for Direct Ocular Exposures - ANSI Z136-1-1976, Table 5|

<sup>4</sup> CLASS 1 ACCESSIBLE EMISSION LIMIT DIVIDED BY AREA OF 80 mm aperture (50.3 cm<sup>2</sup>)

<sup>5</sup> Ratio of calculated corneal or retinal damage (which ever is lower) to BRH CLASS 1 FLUENCE

\* Factor of 100 exception at λ = 1540

† Measured value: 20 J/cm<sup>2</sup> (LAIR)

†† Measured value: 2 J/cm<sup>2</sup> (LAIR)

APPENDIX II  
EYESAFE LASER TRANSCEIVER  
OPERATION AND ALIGNMENT

1.0 GENERAL

The 1.73 $\mu$ m system consists of two assemblies: (a) transceiver unit, containing the laser, laser drive electronics, and receiver; (b) control unit, which houses the power supply and necessary connections. To operate the transceiver, the following ancillary equipment is required:

- i) 24 volt DC power supply
- ii) 15 volt DC power supply
- iii) pulse generator
- iv) oscilloscope

The 24 volt supply is used to drive the inverter which provides the laser bank charge and pockels cell voltages. While the average current required to operate the inverter is low, peak currents of 6-7 amperes are drawn briefly at the onset of charging. The unit should be operated with a supply capable of providing this current if the bank is to be completely charged at a 1Hz repetition rate.

The 15 volt DC supply is used to bias the Germanium photodiode and to provide the receiver operating power. Required current capability for this supply is low,  $\ll 100\text{mA}$ .

The pulse generator must be capable of driving a +5VDC pulse of 50-100 $\mu$ s duration into a 50 $\Omega$  load.

Both high and low ( $50\Omega$ ) impedance oscilloscope preamplifiers have been successfully used to detect the  $t_0$  (outgoing) laser pulse and returns. If the oscilloscope sweep is triggered by the pulse generator driving pulse, the  $t_0$  pulse will occur  $\sim 90\mu\text{s}$  into the sweep, followed by subsequent returns. The  $t_0$  pulse amplitude is typically 300-500mV for a 10mJ outgoing laser pulse.

## 2.0 TRANSCEIVER OPERATION

### 2.1 Connections

Connect the transceiver and control unit using the sheathed main power cable and high voltage BNC cable. IMPORTANT: Never operate the PFN or Q-switch enables unless the transceiver and control unit are connected via the sheathed supply cable and high voltage BNC cable. Unloaded operation of the inverter will damage the unit and will place dangerously high voltages at the open end of the cable.

Connect the 15 and 24 volt power supplies to the appropriate terminals, taking care to observe polarity (Figure 1). The detector/preamplifier is somewhat sensitive to supply voltage transients and the following procedure is recommended: Before connecting the 15 VDC supply, adjust voltage to  $15.0 \pm 0.2$  volts. Shut the supply off, connect, and turn supply on. Connect the pulse generator and oscilloscope. The pulse generator connection is located on the front panel of the control unit; the oscilloscope preamplifier should be connected directly to the detector output cable at the transceiver unit.

### 2.2 Operation

With both the 15 VDC supply and the 24 VDC supply on, turn on the 24 volt on/off switch and PFN charge switch. Operating the

**IMPORTANT:** Never operate unit  
when disconnected from  
transceiver assembly

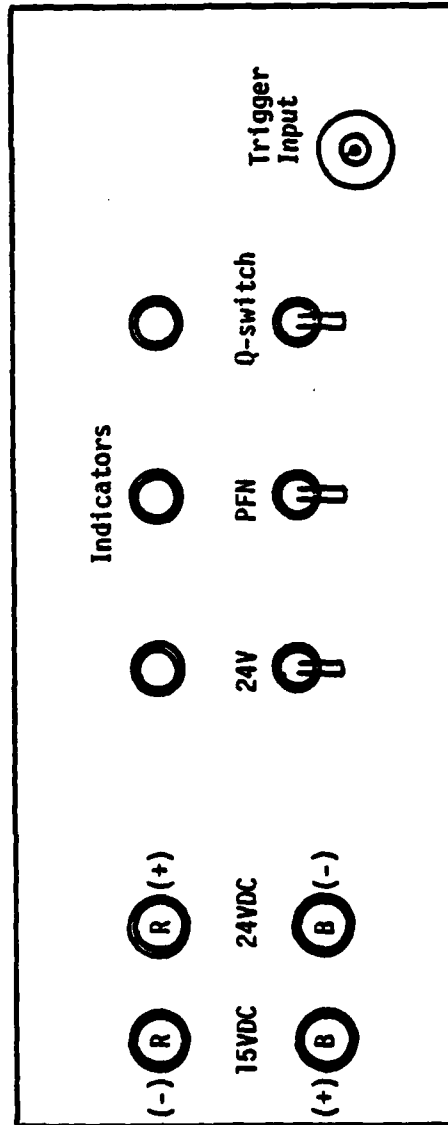


Figure 1. Control Unit Connections

pulse generator will now drive the laser in a long-pulse mode. Turning on the Q-switch enable will allow pulsed operation. When operating at 1Hz a duty cycle of no more than ten pulses, followed by approximately 5 minutes of cool-down time is recommended. To shut down the transceiver, turn the Q-switch and PFN enables off and operate the pulse generator to discharge the bank. Shut off the 24 volt main switch and turn off the 15 VDC and 24 VDC supplies.

### 3.0 TRANSCEIVER ALIGNMENT

#### 3.1 General

Alignment of the transceiver is accomplished via a three-phase procedure: the 1.73 $\mu$ m laser is first aligned, followed by alignment of the transmit-receive optics. Finally, the sighting telescope is boresighted to the optical train.

**CAUTION:** Transceiver alignment involves opening the transceiver case, where high voltage points are accessible to personnel. The flashlamp connections and pockels cell connections should be treated with extreme care. If these connections are to be handled, the system should be off, flashlamp discharged, and all points shorted to ground (transceiver case) through a 25-50K $\Omega$  resistor. Periodic shorting of these points to avoid residual charge accumulation is recommended.

In the following instructions, "left" and "right" refer to the transceiver as viewed from behind, looking in the direction which would be downrange.

#### 3.2 1.73 $\mu$ m Laser Alignment

The following procedure should be followed to align the 1.73 $\mu$ m laser head.

i) Remove the left, right and top transceiver cover plates. The cables passing through the left plate should simply be allowed to slide through the grommets.

ii) Refer to Figure 2. Remove the section of the baseplate containing the dual gold turning mirrors. Remove the 90%R laser coupling mirror from its gimbal by loosening the setscrew.

iii) Pass a He-Ne alignment laser beam through the (now empty) 90%R mirror gimbal and through the Er:YLF laser rod (Figure 2, HeNe position #1). The alignment beam must be centered on both laser rod faces.

iv) Retroreflect the curved rear mirror surface and the Q-switch crystal surfaces to the alignment beam. Re-install the 90% laser mirror and retroreflect its curved surface to the alignment beam.

v) Insert an energy meter and, firing the laser, monitor the Q-switched laser output. This should be  $\geq 15\text{mJ}$  with proper alignment.

vi) Re-install the dual turning mirror assembly. Replace the right side cover.

### 3.3 Transceiver Optics Alignment

i) Reposition the He-Ne laser, directing the beam into the 1.73 laser through the 100%R laser mirror. (Figure 2, HeNe position #2) Adjust the He-Ne laser to pass through the center of both laser rod faces. The He-Ne beam should now be exiting the laser via the 90% mirror, reflecting from the dual gold turning mirrors, and exiting the system via the transmit beam optics. The gold turning mirrors may now be adjusted to center the outgoing He-Ne beam in the negative expanding lens and objective lens.

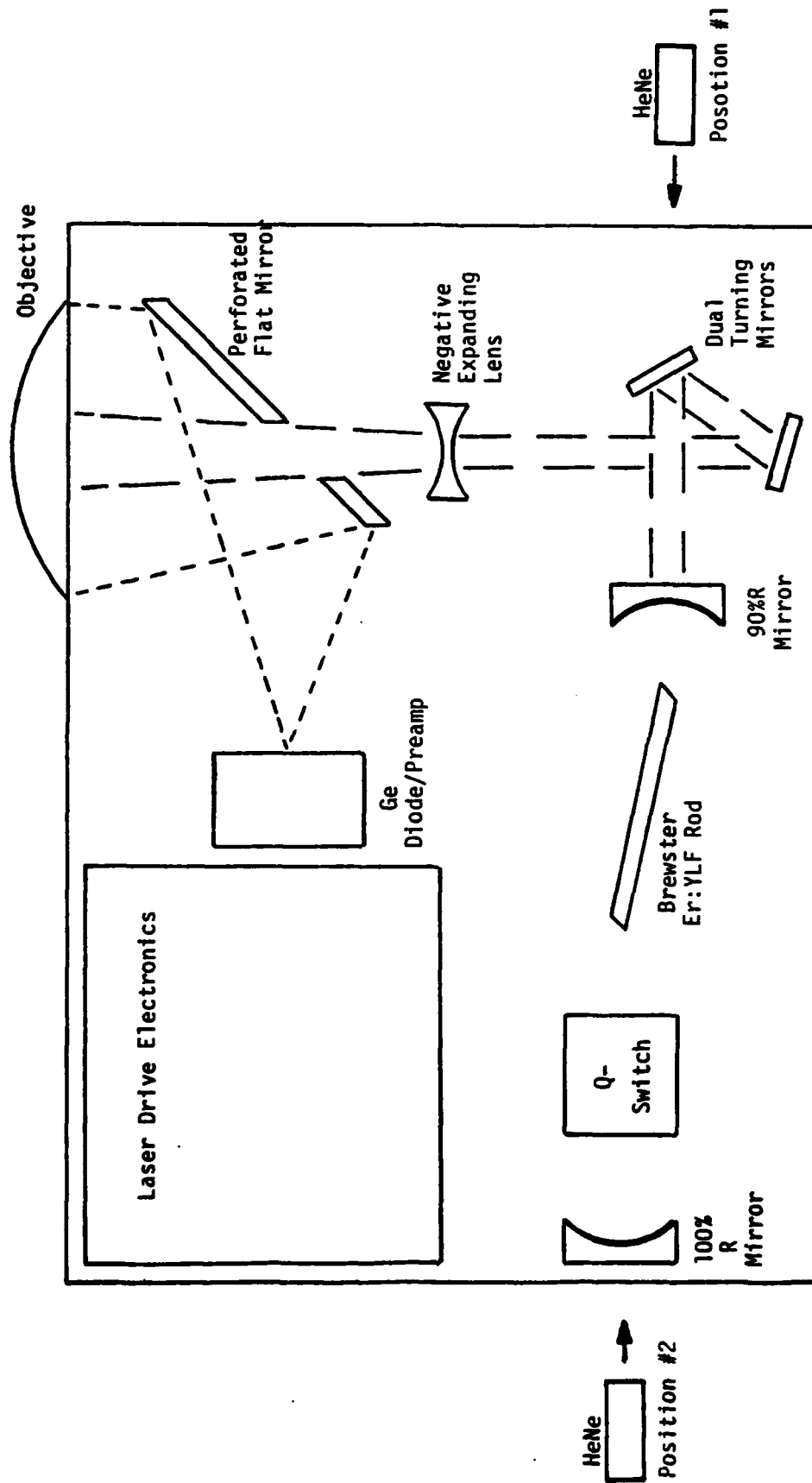


FIGURE 2  
ALIGNMENT LASER POSITIONING

ii) Position the energy meter approximately 25 feet downrange; use the outgoing He-Ne beam to locate the meter. Fire the  $1.73\mu\text{m}$  laser and ensure that the  $1.73\mu\text{m}$  beam impinges on the meter; i.e., that the  $1.73\mu\text{m}$  beam and He-Ne beam are collinear.

iii) Replace the energy meter with an incandescent point source and modulate the source with a chopper. Apply the -15volt input, to power the Ge diode/preamplifier, and couple the preamplifier output into an oscilloscope. Sweep the oscilloscope in a free-running mode, with a horizontal sweep speed commensurate with the chopper frequency.

iv) Adjust the diode/preamplifier positioning to maximize the oscilloscope signal corresponding to the chopped point source. Unless the point source is very bright, the signal will be rather low; a moderately high oscilloscope gain ( $\sim 5\text{mV/division}$ ) will be helpful.

#### 3.4 Sighting Telescope Alignment

The transmit and receive optics are now aligned. Replace the remaining side cover and the transceiver top cover without disturbing the positioning of the receiver. The sighting telescope optical axis is approximately 3" vertically above the objective center; to bore-sight the telescope, measure the exact distance, and align the telescope to a point which is displaced above the point source by this amount.

**DATE**  
**ILME**